Journal of proteome research

Article

Multi-proteomic and transcriptomic analysis of oncogenic #-catenin molecular networks

Rob M. Ewing, Jing Song, Giridharan Gokulrangan, Sheldon Bai, Emily Bowler, Rachel Bolton, Paul Skipp, Yihua Wang, and Zhenghe Wang

J. Proteome Res., **Just Accepted Manuscript** • DOI: 10.1021/acs.jproteome.8b00180 • Publication Date (Web): 10 May 2018

Journal of proteome research

Just Accepted

ACS Publications

is published by the American Chemical Society. 1155 Sixteenth Street N.W., Washington, DC 20036

Journal of proteome research

ACS Publications

is published by the American Chemical Society. 1155 Sixteenth Street N.W., Washington, DC 20036

Graphic

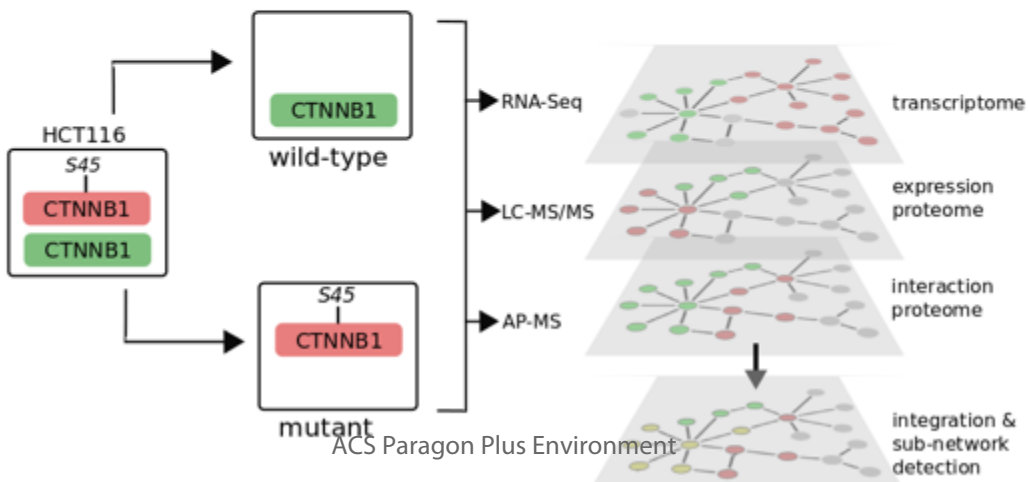

Multi-proteomic and transcriptomic analysis of oncogenic β-catenin molecular networks

Rob M. Ewing[1], Jing Song[2], Giridharan Gokulrangan[2], Sheldon Bai[2], Emily H. Bowler[1], Rachel Bolton[1], Paul Skipp[1], Yihua Wang[1], Zhenghe Wang[2].*

1. School of Biological Sciences, University of Southampton, Southampton, UK
2. School of Medicine, Case Western Reserve University, Cleveland, Ohio, USA

ABSTRACT

Dys-regulation of Wnt signalling is a frequent occurrence in many different cancers. Oncogenic mutations of CTNNB1/β-catenin, the key nuclear effector of canonical Wnt signalling, lead to accumulation and stabilization of β-catenin protein with diverse effects in cancer cells. Although the transcriptional response to Wnt/β-catenin signaling activation has been widely studied, an integrated understanding of the effects of oncogenic β-catenin on molecular networks is lacking. We used Affinity-Purification Mass-Spectrometry (AP-MS), label-free

LC-MS/MS and RNA-Seq to compare protein-protein interactions, protein expression and gene-expression in colorectal cancer cells expressing mutant/oncogenic or wild-type β-catenin. We generate an integrated molecular network and use it to identify novel protein modules that are associated with mutant or wild-type β-catenin. We identify a DNA methyltransferase I (DNMT1) associated sub-network that is enriched in cells with mutant β-catenin and a sub-network enriched in wild-type cells associated with the CDKN2A tumor suppressor linking these processes to transformation of colorectal cancer cells through oncogenic β-catenin signaling. In summary, multi-omics analysis of a defined colorectal cancer cell model provides for a significantly more comprehensive identification of functional molecular networks associated with oncogenic β-catenin signaling.

INTRODUCTION

Altered activity of the Wnt/ β-catenin signaling is a key driver of tumorigenesis in many cancers. Stabilizing mutations of β-catenin are an important class of mutations that alter canonical Wnt signaling and function by blocking phosphorylation of residues that would normally target the protein for destruction [1]. Substitution or deletion mutations at S45 of β-catenin are important clinical mutations in diverse tumors, since this residue acts as a critical molecular switch for canonical Wnt signaling [1,2]. Elevated β-catenin levels then exert oncogenic effects through activation of downstream gene-expression programs in concert with TCF transcription factors [3]. In addition to its role as a transcriptional effector, β-catenin functions as a component of cell-cell adhesion complexes, although the relative balance between β-catenin's different cellular functions is complex [4]. As expected given its diverse functions and sub-cellular localizations, β-catenin exhibits a wide range of different protein

interactions, with other structural proteins in adhesion complexes, proteins in the destruction complex[5], and nuclear interactions with transcription and chromatin modification factors [6]. In addition, transcriptional targets of β-catenin/TCF signalling have been defined in many systems; in cancer cells these include other transcription factors, regulators of the cell-cycle and components and antagonists of the Wnt signaling pathway (Wnt homepage, http://wnt.stanford.edu).

Omics analyses of Wnt activation to date have focused on understanding a single molecular layer of the response to Wnt activation, such as proteomic analyses of selected Wnt pathway components[7,8] or the proteomic or transcriptomic expression response to Wnt activation [9,10]. However, the response to activation of cell signaling pathways occurs at multiple molecular levels; recent work has shown how activation of the Wnt pathway leads directly to protein stabilization in addition to the well-studied transcriptional response [11]. In addition, although it is convenient to consider proximal events in cell signalling (i.e. components of the pathway itself) separately from the response or output of signalling activation (e.g. transcriptional activation), these are intrinsically linked. Several core protein components of the Wnt signaling pathway (e.g. Axin, Dkk) are themselves transcriptional targets, directly activated through β-catenin/TCF signaling and providing feedback regulation of Wnt signaling activity [12,13]

To understand therefore how oncogenic β-catenin alters networks at multiple molecular levels and how this promotes tumorigenesis, we conducted a multi-omics analysis using colorectal cancer cells with targeted inactivation of either the mutant (stabilizing Δ45 mutation) or wild-type allele of CTNNB1/β-catenin [14]. Affinity-Purification Mass-Spectrometry (AP-3

MS) analysis of mutant and wild-type β-catenin cells showed patterns of protein interactions consistent with nuclear localization of mutant β-catenin and membrane-associated wild-type β-catenin. Integrating AP-MS and expression proteomic profiling, we identified several enriched protein networks that are preferentially expressed in mutant or wild-type cells including elevated DNA-methylation linked proteins in mutant cells, and a nucleolar-enriched tumor suppressor module in wild-type cells. Through comparative analysis of enriched Gene Ontology categories, we show that there is concerted alteration of pathways and processes at the proteomic and transcriptomic levels in the mutant and wild-type cells. We show that interaction proteomics, expression proteomics and transcriptomic datasets contribute complementary information to the integrated network, and that multi-omics analysis provides for a more comprehensive delineation of β-catenin associated oncogenesis. In summary, our multi-omics analysis provides a comprehensive view of how oncogenic β-catenin alters molecular networks at multiple levels.

MATERIALS AND METHODS

Cell line culture and sample extraction

Colorectal cancer cell lines HCT116-CTNNB1$^{-/\Delta 45}$ and HCT116-CTNNB1$^{WT/-}$ were regularly maintained in McCoy-5A media (Life Technologies, 16600-108, Carlsbad, CA) containing 10% fetal bovine serum (Life Technologies, 10438-026, Carlsbad, CA) and 1% streptomycin-penicillin (Life Technologies, 15140-148, Carlsbad, CA) at 37°C in CO2 incubator (5% CO2, 100% H2O). Cells were harvested by scraping the cells off plates and then washed with cold PBS twice for immediate use or storage (-80°C). Harvested cells were lysed (25mM Tris-HCl, pH7.4, 1mM EDTA, 150mM NaCl, 1% NP-40, 50% glycerol, Protease

inhibitor cocktail) by homogenization and incubated on ice for 30 min followed by centrifugation at 13,000rpm for 30min. The supernatant (soluble fraction) was kept for further analysis. Proteins were quantified by Bio-Rad protein assay dye (500-0006, Bio-Rad, Hercules, CA) by measuring the absorbance at 595nm. NE-PER Nuclear and Cytoplasmic Extraction kit (Pierce) was used to prepare nuclear and cytosolic fractions, which were assessed using anti-Dnmt1 and anti-Gapdh Western blots.

SDS-PAGE & Immunoblotting

Equal amounts (20 μg) of proteins from different samples was loaded on precast 4−12% Bis-Tris gel (Life Technologies NP-0335, Carlsbad, CA) and subjected to electrophoresis. Gels were either stained with Coomassie Brilliant Blue (Pierce 20278, Rockford, IL) or transferred to nitrocellulose membrane (Whatman 10402594, Dassel, Germany). Western blotting was used to detect the protein with super signal ELISA Pico chemiluminescent substrate. Primary antibodies used: anti-β-catenin (Cell Signaling Technology 9581, Danvers, MA), anti-Dnmt1 (Cell Signaling Technology 5119, Danvers, MA), anti-UHRF1 (Novus Biologicals H00029128-M01, Littleton, CO), anti-HDAC1 (Abcam ab7028, Cambridge, MA), anti-PCNA (Santa Cruz Biotechnology sc-56, Santa Cruz, CA) and anti-α-tubulin (Cell Signaling Technology, Inc., 2144, Danvers, MA). Loading controls were applied at 1:1000 and secondary antibodies horseradish peroxidase (HRP)-conjugated anti-mouse (Promega W4011, Madison, WI) and HRP-conjugated anti-rabbit (Cell Signaling Technology 7074, Danvers, MA) were added at 1:20,000. Chemi-luminescence detection using SuperSignal* ELISA Pico Chemiluminescent Substrate (Thermo Scientific PI-37070, Rockford, IL) was applied to all westerns.

Proteomic sample preparation

For analysis of the expression proteome, cell extracts were fractionated using the NE-PER Nuclear and Cytoplasmic Extraction kit (Pierce), each fraction separated using SDS-PAGE and then fractionated in 2 fractions per sample/lane after Coomassie blue staining prior to tryptic digestion. Each sample combination (e.g. Mutant/nuclear, Mutant/cytosolic) was replicated twice. Affinity-purifications from 10^7 cells were performed as previously described [15] using anti-β-catenin (Cell Signaling Technology 9581, Danvers, MA) antibodies. Affinity-purification experiments were replicated using two independent mutant and two independent wild-type cell lines, and each sample replicated twice. In-gel tryptic digestion was performed and combined elution fractions were lyophilized in a SpeedVac Concentrator (Thermo Electron Corporation, Milford, MA), resuspended in 100 µL of 0.1% formic acid and further cleaned up by reverse phase chromatography using C18 column (Harvard, Southborough, MA). The final volume was reduced to 10µL by vacuum centrifugation and addition of 0.1% formic acid.

Mass-spectrometry

Online reverse phase nanoflow capillary liquid chromatography (nano-LC, Dionex Ultimate 3000 series HPLC system) coupled to electrospray injection (ESI) tandem mass spectrometer (Thermo-Finnegan LTQ Orbitrap Velos) was used to separate and analyze tryptic peptides. Peptides were eluted on nano-LC with 90 min gradients (6 to 73% acetonitrile in 0.5% formic acid with a flow rate of 300 nL/min). Data dependent acquisition was performed using Xcalibur software (version2.0.6, Thermo Scientific) in positive ion mode with a resolution of 60 000 at m/z range of 325.0−1800.0, and using 35% normalized collision energy. Up to the five most intensive multiple charged ions were sequentially isolated, fragmented and further analyzed. Raw LC-MS/MS data were processed using Mascot version 2.2.0 (Matrix Science, Boston,

MA). The sequence database was searched with a fragment ion mass tolerance of 0.8Da and a parent ion tolerance of 15 ppm. The raw data were searched against the human International Protein Index database (74,017 protein sequences; version 3.42) with fixed modification carbamidomethyl (C) and variable modification oxidation (M), and 1 allowed missed cleavage. Peptides were filtered at a significance threshold of $P < 0.05$ (Mascot). Raw mass spectrometry chromatograms were processed and analyzed using Xcalibur Qual Browser software (Thermo Fisher Scientific Inc. Version 2.0.7). Scaffold (Proteome Software Inc., Portland, OR, USA; version 3.00.04) was used to analyze LC-MS/MS-based peptide and protein identifications. Peptide identifications were accepted if they could be established at greater than 95.0% probability as specified by the Peptide Prophet algorithm [16]. Protein identifications were accepted if they could be established at greater than 99.0% probability and contained at least 2 identified peptides. Proteins that contained similar peptides and could not be differentiated based on MS/MS analysis alone were grouped to satisfy the principles of parsimony. Protein quantitation for the expression proteomics study was performed using ion peak intensity measurements in the Rosetta Elucidator software (version 3.3.0.1; Rosetta Inpharmatics LLC, Seattle, WA). The PeakTeller algorithm within Rosetta Elucidator was used for peak detection, extraction and normalization of peptide and protein abundance. Protein quantitation of AP-MS experiments was performed using Scaffold (Proteome Software Inc., Portland, OR, USA; version 3.00.04) to compute normalized spectral counts for each protein. Proteins were excluded from AP-MS results if frequency across control experiments from HCT116 cells was > 0.33 [15]. Mass spectrometry data are available via the PRIDE repository with dataset identifiers PXD006053 (Expression proteome) and PXD006051 (Interaction proteome).

RNA-Seq Analysis

The quantity of total RNA in each sample was collected using Qubit (Invitrogen) and libraries prepared using Illumina TruSeq Total RNA v2 kit with Ribo Zero Gold for rRNA removal. The Ribo-Zero kit was used to remove ribosomal RNA (rRNA) from 1 μg of Total RNA using a hybridization/bead capture procedure that selectively binds rRNA species using biotinylated capture probes. The resulting purified mRNA was used as input for the Illumina TruSeq kit in which libraries are tagged with unique adapter-indexes. Final libraries were validated using the Agilent High Sensitivity DNA kit (Agilent), quantified via Qubit, and diluted and denatured per Illumina's standard protocol. High-throughput sequencing was carried out using the Illumina HiScan SQ instrument, 100 cycle paired-end run, with one sample loaded per lane, yielding on average > 100 million reads per sample. Reads were mapped to human genome hg19 using TopHat2 version 2.1.0 [17] with default settings and reads summarized by gene feature using htseq-count . Differential expression analysis was performed and p-values adjusted for fdr were computed with DeSeq. Data are available from GEO, accession: GSE95670.

Functional and network analyses

The Combined Abundance Score as previously described [19] was computed using all significant ($p<0.05$) proteins from the 3 datasets, providing a single, normalized log fold change value for each protein. (Selected additional protein were included where the p-value was significant at $p<0.1$, since it was observed for several proteins that they were differentially abundant across more than one dataset – e.g. CUL1). Functional networks were constructed from the Pathway Studio database (Elsevier), version 9.0. Gene/Protein identifiers were imported and networks created by selecting all direct edges between the imported nodes

(Physical Interactions, Expression Regulation and Protein Modification relations. Network diagrams were created in Cytoscape (v3.3.0). Edge thickness between two functional groups was calculated by dividing the number of interactions between the groups by the size of the groups (number of genes/proteins) creating a normalized edge weight. Gene Ontology term enrichment was computed in Pathway Studio (Ariadne Genomics). The significantly differential sets of mutant and wild-type genes from the RNA-Seq analysis were analyzed using Enrichr [20] and o-POSSUM-3 [21].

Experimental Design and Statistical Rationale

Affinity-Purification Mass-Spectrometry (AP-MS) were performed on two independently derived clones of the HCT116-CTNNB1$^{-/\Delta 45}$ and HCT116-CTNNB1$^{WT/-}$cell-lines (i.e. 4 different cell-lines) and then replicated twice. The use of independent clones allowed us to capture the biological variation in the expression of CTNNB1/β-catenin. We observed that AP-MS proteomics experiments produced very similar results between these clones (Supplementary Figure 1). Expression Proteomics experiments were performed on sub-cellular fractionated mutant and wild-type cell cultures. Each combination of cell-type/sub-cellular fraction (mutant/nuclear, mutant/cytosol, wild-type/nuclear, wild-type/cytosol) was replicated twice, and we found high correlation within these groups (Supplementary Figure 3). RNA-Seq experiments were performed in triplicate (3 mutant, 3 wild-type), yielding significant differentially regulated transcripts at low fdr. For each dataset, the $\log_2$ ratio of mutant/wild-type abundance was computed and Student's T-test was used to compute p-values with adjustment for false discovery rate.

RESULTS

Experimental overview

The experimental strategy of this study is to use multiple, complementary 'omics approaches to identify perturbed molecular networks as shown in Figure 1. We used a previously described model derived from HCT116 colorectal cancer cells (heterozygous for stabilizing Δ45 mutation of β-catenin) in which either the mutant or wild-type allele has been disrupted [14] thus creating two cell-lines expressing either mutant β-catenin ($CTNNB1^{-/\Delta 45}$) or wild-type β-catenin ($CTNNB1^{WT/-}$). To characterize mutant and wild-type β-catenin protein-protein interactions we used anti-β-catenin Affinity-Purification Mass-Spectrometry (LC-MS/MS AP-MS). We also analyzed nuclear and cytosolic fractions to increase overall coverage using label-free protein profiling (LC-MS/MS) to identify differentially abundant proteins in the mutant and wild-type cells (2 replicates of each cell-type/fraction combination – a total of 8 samples). Finally, we used RNA-Seq (Illumina HiSeq) to compare the transcriptomes of mutant and wild-type β-catenin cells. Three replicates of each of mutant and wild-type were analyzed and genes with differential gene-expression profiles identified.

AP-MS analysis identifies distinct mutant and wild-type β-catenin protein interactions

We analyzed the mutant and wild-type β-catenin protein interactions using AP-MS experiments as shown in Figure 2. AP-MS analyses were performed using two distinct clones each for mutant and wild-type cells (a total of 4 replicates of mutant and 4 replicates of wild-type cells), and we observed high correlation of protein abundance in AP-MS analyses between replicates and clones (Supplementary Figure 1). AP-MS experiments yielded 67 proteins

differentially associated with mutant or wild-type β-catenin ($p<0.05$), and we observed distinct profiles of proteins from the mutant and wild-type AP-MS analyses that are consistent with the differential sub-cellular localization of mutant and wild-type β-catenin (Supplementary Table 1). Figure 2A shows a heatmap of proteins significant proteins identified in AP-MS experiments and Figure 2B a volcano plot of $\log_2$ ratios of mutant and wild-type proteins. We found that mutant protein interactions were highly enriched for nuclear proteins and for proteins functioning in regulation of gene-expression, whereas wild-type proteins were significantly enriched for membrane-associated proteins (see Figure 3). To investigate in more detail, we constructed a protein network of all known physical interactions between the identified set of proteins. The largest connected component of this network is shown in Figure 2C with known mutant-enriched (red) and wild-type-enriched (green) β-catenin interaction partners identified in the analysis. Higher interconnectivity between pairs of proteins identified in the mutant cells was observed than between proteins identified in the wild-type cells (and this is not due to differences in the overall connectivity of mutant- and wild-type-enriched proteins, as there is no significant difference between the degree distributions of the mutant and wild-type proteins: two sample t-test; p-value > 0.3). These findings and the distinct sets of enriched functional categories indicate that β-catenin in the mutant and wild-type cells functions in distinct protein networks, in concordance with distinct sub-cellular localizations of mutant and wild-type β-catenin.

Comparison of functional trends between mutant and wild-type cells

We next analyzed gene and protein expression in the mutant and wild-type cells using RNA-Seq and LC-MS/MS respectively. RNA-Seq analysis identified transcripts from 18239 genes

with 1085 showing significantly differential expression in mutant cells ($p<0.05$; log-fold-change >2) and 735 showing significantly differential expression in wild-type cells (FPKM distribution plots, Supplementary Figure 2). To increase protein coverage, we performed protein expression profiling in conjunction with sub-cellular fractionation of cell lysates. This analysis yielded 640 proteins identified as significantly differentially expressed ($p<0.05$) between mutant and wild-type cells in either cytosolic or nuclear fractions. We compared the functional trends in the interaction proteome, expression proteome and transcriptome datasets. For each dataset, Gene Ontology (GO) terms significantly ($p<0.05$) enriched in mutant and/or wild-type samples were identified and then compared across the datasets. Overlap of significantly differential genes/proteins between the datasets was limited (57 genes/proteins were identified in more than one dataset from a combined total of 2465 significantly differentially regulated genes or proteins). However, significant numbers of shared enriched GO terms were identified across all 3 datasets. The number of shared GO terms is summarized in Figure 3A, and we observed much greater concordance between mutant-enriched GO terms between datasets and between wild-type-enriched GO terms, indicating a concerted cellular response at proteomic and transcriptomic levels to β-catenin mutation (Figure 3A). Selected significantly enriched GO terms in either mutant or wild-type cells are shown in Figure 3B, and these reflect the findings for the AP-MS dataset, whereby mutant transcriptome and proteome datasets are enriched for nuclear and gene-expression associated functions, whereas the wild-type transcriptome and proteome are enriched for membrane and cytoskeleton associated functions. In addition, comparison of the differentially regulated RNA-Seq gene sets against two curated repositories, TSGene [22] and the Tumor Associated Gene database [23], showed significant enrichment ($p=0.00182$; Fisher's Exact) of tumor suppressors and

oncogenes (p=0.02979; Fisher's Exact), indicating that these cancer-relevant functional classes are frequently differentially regulated in the mutant/wild-type β-catenin model.

As expected, the GO analysis showed that canonical Wnt signaling was highly enriched in the mutant cells. We therefore analyzed which direct canonical Wnt signaling targets (taken from the Wnt homepage http://wnt.stanford.edu), bound by TCF transcription factors were differentially expressed between mutant and wild-type cells (Supplementary Table 2), and found that many of the known Wnt targets are differentially regulated in our data, indicating a substantial direct response to β-catenin/TCF. We noted that two classical targets of canonical Wnt signaling CCND1 (cyclin D1) and MYC (c-myc) were not significantly differential between the mutant and wild-type cells. The same finding was reported in the initial analysis of the same cell-lines, and it was concluded that although these genes have been observed as direct transcriptional targets of β-catenin/TCF in many systems [24], they are not physiological targets in these cell-lines [14]. We next compared our transcriptome dataset to two previously published CTNNB1 siRNA analyses in colorectal cancer cells [25,26]. This previous study identified a set of 335 genes for which a consistent positive and negative trend was seen across siRNA experiments in 2 colorectal cancer cell-lines. Comparing our transcriptome dataset to this set showed a significant overlap and trend correlation (p=0.0245; Fisher's Exact Test), in particular in the correlation between genes whose expression is repressed in response to CTNNB1 siRNA and genes up-regulated in mutant CTNNB1 cells (Supplementary Table 3), indicating that different β-catenin perturbation models (siRNA, knock-out) have similar transcriptional outcomes.

To further understand the transcriptional regulatory programs in the mutant or wild-type cells, we analyzed enriched transcription factor binding sites in the mutant or wild-type gene sets (Figure 3C). The β-catenin binding partner Lef1, a TCF transcription factor is amongst the most highly represented predictions in the mutant cells. We also noted that the mutant and wild-type gene sets exhibited enrichment of different classes of transcription factor (Figure 3C).The wild-type set is highly enriched in zinc-finger transcription factor binding sites (6/10 of the top 10 most enriched TFs are of this type). Multiple Kruppel-like factor (KLF) transcription factors are represented in this set, and this class of transcription factor have been shown to function as tumor suppressors in colorectal cancer [27–29]. KLF4 has been shown to interact with Beta-catenin and inhibit Wnt signaling in the colon [30,31]. TCF3 is also identified as an enriched transcription factor in the wild-type cells. Recent analysis showed that TCF3 binds the MYC Wnt-responsive element to inhibit MYC expression by preventing binding of β-catenin/TCF4 at the same promoter element [32].

An integrated proteomic and transcriptomic network

To construct an integrated network combing the transcriptome, expression proteome and interaction proteome data, a combined abundance score [19] was computed for each significant node (p-value <0.05) across the three datasets. All direct relations (physical interaction, protein modification and expression regulation) between the 2623 gene/protein entities in the combined set were used to construct an integrated network using the Pathways Studio database (we use hereafter the terminology ‘edge’ to refer to protein-protein relations and ‘node’ to refer to proteins themselves). To analyze how each of the omics datasets contributes to this integrated network, we computed several network statistics (Figure 4). We observed that the

average degree of nodes from each of the three datasets differ within the integrated network (interaction proteome=5.95; expression proteome=7.62; transcriptome=3.98) and we therefore plotted the degree distributions of nodes from each dataset as shown (Figure 4B). Nodes within the transcriptome dataset have a distinctly lower average degree, attributed to the large fraction of genes/proteins from this dataset with few described interactions in the database. The significant enrichment of genes encoding transcription factors present in the significantly differential transcriptome dataset contributes towards this difference since for many of these genes, relatively few interactions have been described. This finding prompted us to investigate whether the types of edges represented in the 3 datasets differed (Figure 4C). We observe substantial differences in edges annotated as 'Binding' in the Pathway Studio database and those annotated as regulating 'Expression', with greater numbers of Binding edges in the interaction and expression proteome datasets and substantially more Expression edges in the transcriptome dataset, indicating the complementarity these different omics datatypes in identifying different types of proteins and edges.

Functional module identification and validation

To focus on specific modules within the integrated network, we curated sub-networks associated with biological pathways or processes that were identified as significantly different between mutant and wild-type cells in the gene set enrichment analysis. Figure 5A shows several selected modules within the integrated network with β-catenin-associated functions. The abundance of proteins indicative of epithelial-mesenchymal transition (EMT) were strongly enriched in the mutant cells. We noted that epithelial markers such as claudins and E-cadherin were differentially expressed in the wild-type cells [33], whereas mesenchymal markers

such as the cytoskeletal protein Vimentin (VIM) are strongly enriched in the mutant cells (VIM was differentially expressed in both the expression proteome and transcriptome datasets). In addition, several proteins with functions in tissue remodelling such as matrix metalloprotease (MMP13) and laminins (LAMB3, LAMC2) which form the basement membrane required for attachment and organization of epithelial cells were identified.

Wild-type cells preferentially expressed proteins implicated in non-canonical Wnt signaling. In addition to non-canonical Wnt ligands WNT5A and WNT7A, we found that the Dishevelled (Dvl) -interacting proteins, DACT3 and DAAM1 were more abundant in the wild-type cells. DACT3 is a member of a family of proteins known to antagonize canonical Wnt/β-catenin signaling, suggesting that the process of mutant β-catenin-driven oncogenesis involves repression of antagonists of canonical signalling. Whilst most components of TGF-Beta/SMAD and BMP signaling were higher in mutant cells (module 7), we noted that LEMD3, a known antagonist of TGF-Beta/SMAD signaling was significantly higher in wild-type cells.

Although integration of transcriptomic and proteomic allowed for increased coverage and representation within functional modules as shown in Figure 5A, we also observed exclusively proteomic modules. Skp-Cullin-Fbox (SCF) protein complexes are ubiquitin ligase complexes that regulate ubiquitination of many proteins including β-catenin, and these were uniformly more abundant in mutant cells (Figure 5B). This module was almost uniformly significantly differentially regulated in the proteomic datasets, but not in the transcriptomic dataset,

indicating, in concordance with other findings, that these complexes are mainly regulated at the post-translational level, through dynamic re-arrangement of protein components [34].

We selected two modules for further validation (Figures 5C and 5D). The primary maintenance DNA methyltransferase (DNMT1) is significantly more abundant in the expression proteome and transcriptome of mutant cells. We analyzed the expression of Dnmt1 and two direct interaction partners of Dnmt1, USP7/HAUSP and UHRF1 and all of these proteins were found to be both nuclear specific and enriched in mutant cells (Figure 5C). We previously showed that an interaction between β-catenin and the primary DNA methyltransferase, Dnmt1 stabilizes both proteins in the nucleus of cancer cells [35]. We previously showed that USP7 regulates the stability of Dnmt1 in cancer cells [36], and UHRF1 has been shown to also participate in the regulation of Dnmt1 stability via ubiquitination [37]. These latest results indicate the coordinated up-regulation of Dnmt1-USP7-UHRF1 complexes in mutant cells, linking β-catenin-driven oncogenesis to altered DNA methytransferase activity.

We also noted that one of the most enriched categories in the gene enrichment analysis for WT cells were proteins annotated as nucleolar (WT expression proteome dataset, p-value=$4x10^{-11}$), and with the related functional annotations of rRNA processing and ribosome biogenesis. We found that many of these proteins formed a highly-connected module within the larger integrated network (Figure 5D). Western analysis was used to validate the expression of several proteins that were either significantly differentially abundant in the omics datasets (shaded green) or predicted based upon their connections to other proteins in the module (shaded gray).

In addition to their role in ribosome function, several of these proteins have known tumor-suppressor functions. The well-characterized tumor suppressor CDKN2A (P19ARF) is a prominent member of this module and functions to regulate the levels of p53 through its sequestration of MDM2 (a negative regulator of p53) [38] in the nucleolus (MDM2 was not identified in the proteomic experiments, and not significantly differentially expressed in the transcriptomic experiments). Another protein, nucleostemin (GNL3) that has also been linked to MDM2-p53 regulation [39] was differentially more abundant in wild-type cells. We previously identified GNL3 as an interaction partner of LYAR [40], and therefore analyzed the expression of this and several other known nucleolar proteins linked to LYAR as shown in Figure 4D, showing their greater abundance in wild-type cells.

DISCUSSION

In this study, we performed the first multi-proteomic and transcriptomic analysis of the molecular response to stabilization of β-catenin in colorectal cancer cells. We used a cell model of oncogenic β-catenin activity to compare cells expressing a pathogenically and clinically important β-catenin mutation that stabilizes the protein with cells expressing wild-type β-catenin. Global analysis of functional trends showed that mutant cells and mutant β-catenin interactions were enriched in mutant cells in line with the known importance of nuclear accumulation of β-catenin for its pathogenic activity. This is in line with the findings presented in the original publication describing these cells showing that β-catenin in the mutant cells was

more abundant in the nucleus, and bound less to E-cadherin than β-catenin in the wild-type cells, even though the overall abundance of β-catenin in the two cell-lines was similar [4]

Using integrated proteomic and transcriptomic analyses allowed us to reveal novel functional modules associated with β-catenin-driven oncogenesis. Significantly differential expression of multiple Wnt ligand genes was observed between mutant and wild-type cells. WNT2, WNT5A and WNT7A are significantly higher in the wild-type cells whereas WNT16 is higher in mutant cells. Wnt5a is the best studied ligand of this group and is associated with β-catenin-independent or non-canonical Wnt signalling [41]. Interestingly, WNT5A can antagonize β-catenin signalling [42], exhibits tumor suppressive activity in colorectal cancer [43] and is associated with sub-groups of colorectal cancer patients with good prognosis [44], although WNT5A's tumor suppressor properties appear to be limited to certain tumor types [41]. We also showed that the expression of DNA methyltransferase I (Dnmt1) and several key Dnmt1 interaction partners are significantly elevated in mutant β-catenin cells, consistent with our previous report that β-catenin and Dnmt1 proteins engage in a mutually stabilizing interaction in the nuclei of cancer cells [35]. In addition, USP7 which regulates the stability of Dnmt1 has also recently been shown to stabilize β-catenin in colorectal cancer cells expressing APC mutations [45], further linking the regulation of Dnmt1 to β-catenin-driven oncogenesis. Conversely, we identified a module of nucleolar-enriched proteins that were significantly more abundant in wild-type β-catenin cells, including the tumor suppressor CDKN2A. Expression of CDKN2A is frequently silenced in colorectal and other tumors through promoter hyper-methylation [46], suggesting that alterations of CpG methylation may be induced via oncogenic β-catenin and the greater

abundance of DNMT1 and its associated regulators that we observed in cells with mutant β-catenin.

Our study showed how a multi-omics approach combining different layers of proteomic and transcriptomic information can reveal more comprehensively how oncoproteins transform molecular networks in cancer cells. Recent studies have shown that in addition to mediation of a transcriptional response, activation of canonical Wnt signaling also acts in-dependently of transcriptional programs to alter protein stabilization [47], necessitating the characterization of oncogenic-mediated effects at proteomic as well as transcriptomic levels. We have adopted the approach of integrating multi-omics data with existing network information [48] to identify modules within the cellular network that may be perturbed across the multiple layers of transcriptome, expression proteome or interaction proteome. We observed concerted cellular responses in terms of pathways and processes across these multiple layers. We also showed that these different 'layers' of information contribute differentially to the overall analysis of β-catenin-driven oncogenesis – by for example contributing different types of protein-protein relationship (edges) and identifying proteins with differing network features. In summary, our study reveals both novel biology associated with β-catenin-driven oncogenesis and also illustrates the greater insight that can be gained from applying a systematic multi-omics approach.

Figure 1

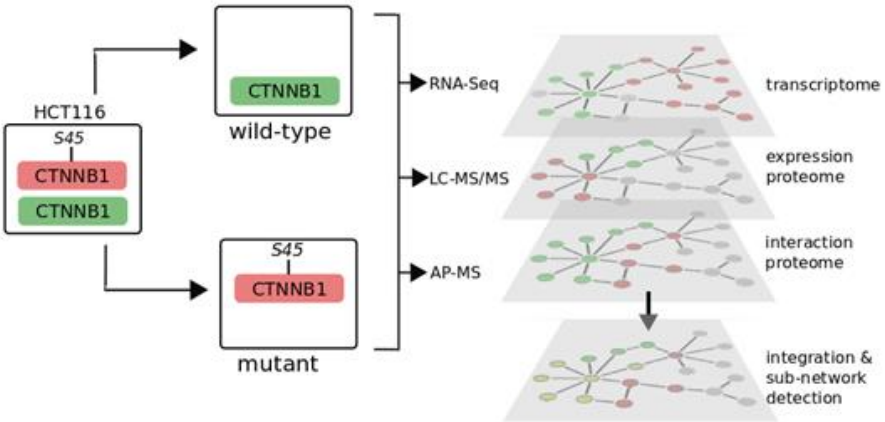

Figure 1 Integrated multi-omics analysis of β-catenin signalling networks Experimental design and data acquisition of interactome (AP-MS), expression-proteome (LC-MS/MS) and transcriptome (RNA-Seq) from colorectal cancer cell lines HCT116-CTNNB1$^{-/\Delta 45}$ (mutant) and HCT116-CTNNB1$^{WT/-}$ (wild-type) expressing endogenous mutant or wild-type CTNNB1/β-catenin.

455

Figure 2

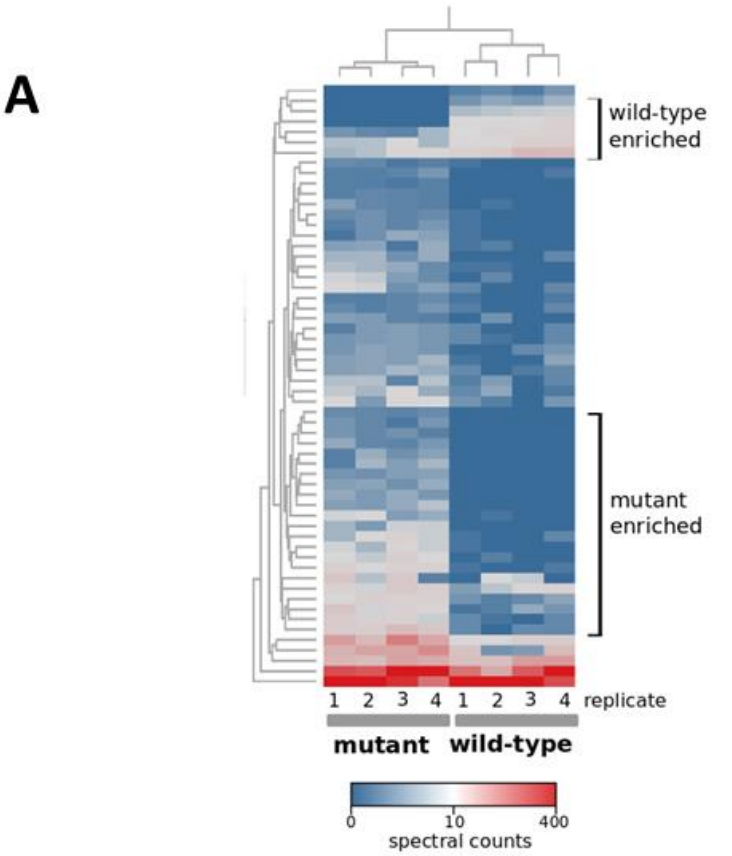

456

Figure 2 (cont'd)

C

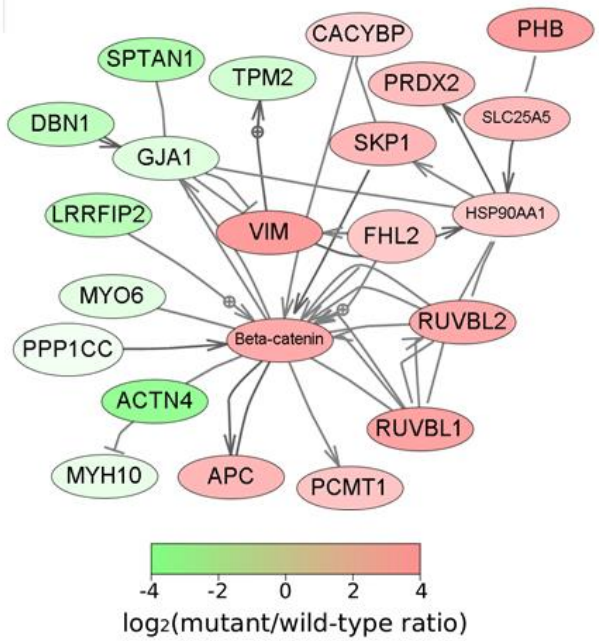

457 **Figure 2 Affinity-Purification Mass-Spectrometry (AP-MS) analysis of mutant and wild-**

458 **type β-catenin protein interactions**(A) Heatmap of protein spectral counts across 4 replicate

459 HCT116-CTNNB1$^{-/\Delta 45}$ (mutant) and 4 HCT116-CTNNB1$^{WT/-}$ (wild-type) AP-MS samples.

Selected profiles of proteins associated with either mutant AP-MS or wild-type AP-MS samples are shown.

(B) Volcano plot indicating $\log_2$ ratio of mutant/wild-type spectral counts from single AP-MS study, with significantly ($p<0.05$) proteins indicated.

(C) Network diagram of β-catenin (CTNNB1) interaction partners identified in the study. The largest connected component sub-network in the Pathway Studio analysis is shown. Proteins are shaded according to their mutant/wild-type spectral count ratio (red proteins are highly enriched in mutant AP-MS samples, green shaded proteins are highly enriched in wild-type AP-MS samples).

Figure 3

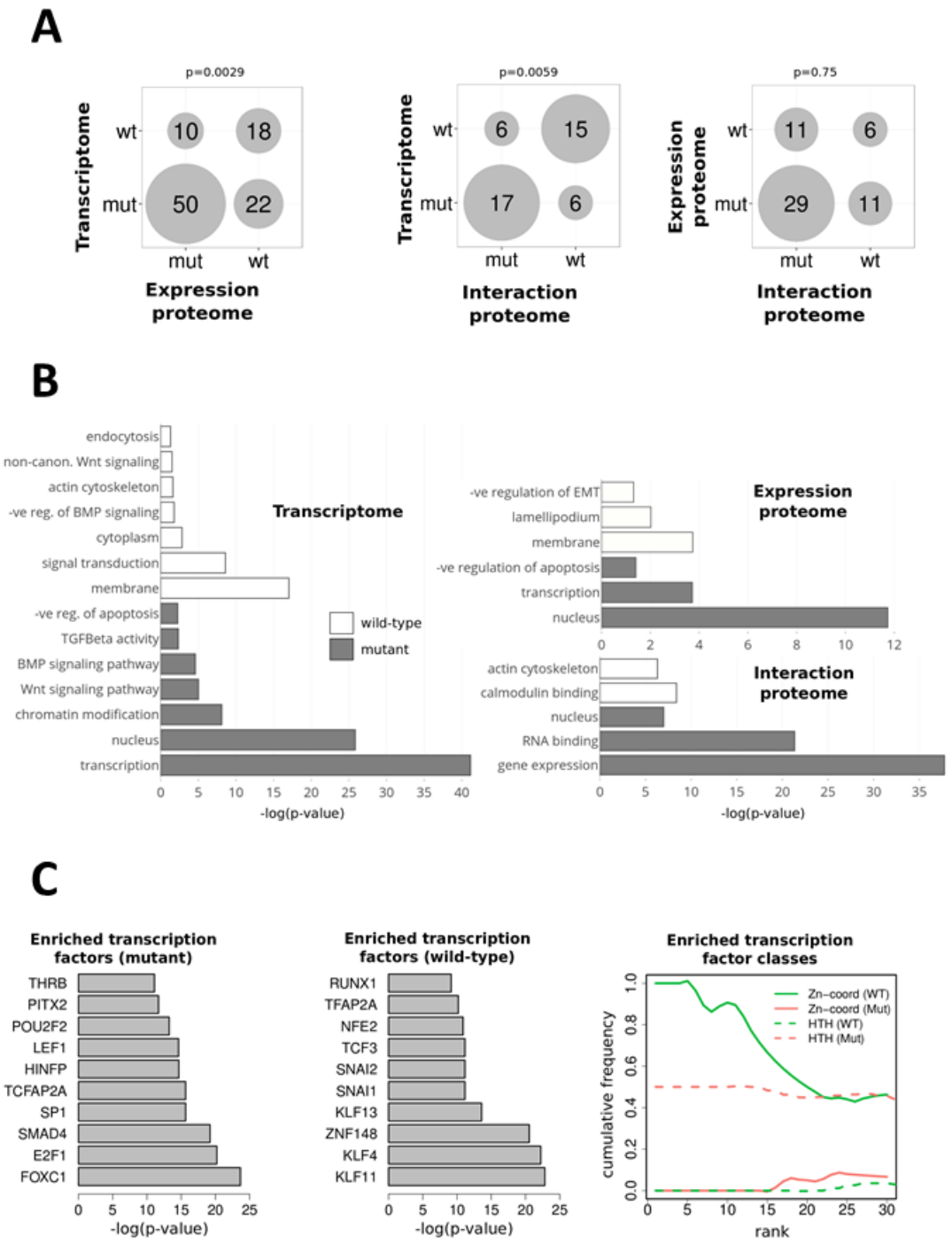
A
p=0.0029
Transcriptome
wt
mut
10
18
50
22
mut
wt
Expression proteome
p=0.0059
Transcriptome
wt
mut
6
15
17
6
mut
wt
Interaction proteome
p=0.75
Expression proteome
wt
mut
11
6
29
11
mut
wt
Interaction proteome
B
endocytosis
non-canon. Wnt signaling
actin cytoskeleton
-ve reg. of BMP signaling
cytoplasm
signal transduction
membrane
-ve reg. of apoptosis
TGFBeta activity
BMP signaling pathway
Wnt signaling pathway
chromatin modification
nucleus
transcription
Transcriptome
wild-type
mutant
0 5 10 15 20 25 30 35 40
-log(p-value)
-ve regulation of EMT
lamellipodium
membrane
-ve regulation of apoptosis
transcription
nucleus
Expression proteome
0 2 4 6 8 10 12
actin cytoskeleton
calmodulin binding
nucleus
RNA binding
gene expression
Interaction proteome
0 5 10 15 20 25 30 35
-log(p-value)
C
Enriched transcription factors (mutant)
THRB
PITX2
POU2F2
LEF1
HINFP
TCFAP2A
SP1
SMAD4
E2F1
FOXC1
0 5 10 15 20 25
-log(p-value)
Enriched transcription factors (wild-type)
RUNX1
TFAP2A
NFE2
TCF3
SNAI2
SNAI1
KLF13
ZNF148
KLF4
KLF11
0 5 10 15 20 25
-log(p-value)
Enriched transcription factor classes
Zn-coord (WT)
Zn-coord (Mut)
HTH (WT)
HTH (Mut)
cumulative frequency
0.0 0.2 0.4 0.6 0.8 1.0
0 5 10 15 20 25 30
rank

Figure 3 Functional analysis of β-catenin-associated proteomic and transcriptomic profiles

(A) Bubble plot indicating the size of the intersections of Gene Ontology terms between interaction, expression proteome and transcriptomic datasets. The numbers indicate shared GO terms for each comparison, for GO terms significantly ($p<0.05$) enriched in mutant or wild-type samples. p-values are Fisher's Exact Test indicating the significance of the observed overlap of GO terms.

(B) Enriched Gene Ontology (GO) terms in mutant and wild-type cells across each dataset. The most significantly differential GO terms were identified for each dataset by comparing the p-values for each term between mutant and wild-type gene-sets.

(C) Enriched transcription factors in the significantly ($p<0.05$) differential mutant or wild-type gene sets from RNA-Seq analysis. Enrichr analysis was used to identify the most enriched transcription factors in the significantly differential ($p<0.05$) RNA-Seq datasets. The top 10 enriched transcription factors are shown for mutant and wild-type (panel 1 and 2). Ranked transcription factor classes for the mutant and wild-type RNA-Seq significantly differential datasets showing distinct classes of transcription factors in each cell-type.

Figure 4

A

	Interaction proteome	Expression proteome	Transcriptome
Nodes	345	549	1633
Edges	2053	4186	6501

B

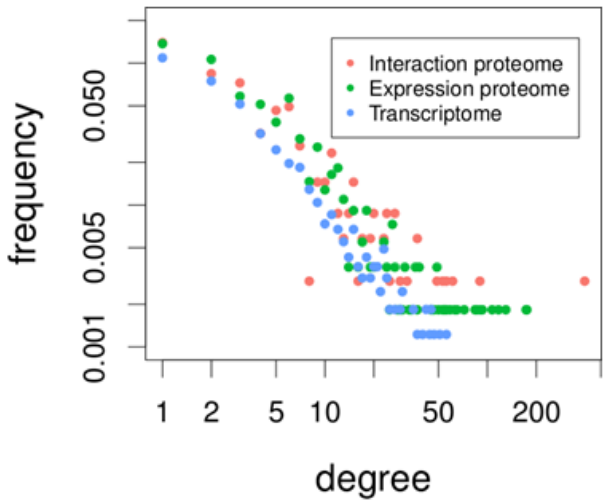

C

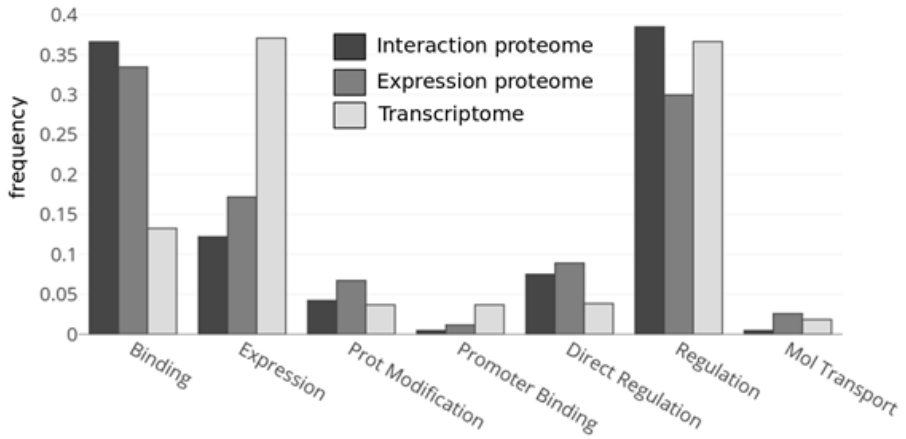

488

489

Figure 4 Network properties of proteomic and transcriptomic datasets

(A) Summary of network properties from the integrated network constructed by integrating all 3 datasets with known protein-protein interactions. The table indicates the numbers of nodes (protein/genes) and edges (relations between proteins) from each dataset integrated into the combined network.

(B) Log-log plot of the degree distributions for nodes from each dataset (Number of connections for protein nodes typically show interaction proteome > expression proteome > transcriptome).

(C) Analysis of interaction (edge) types for each dataset indicate significant differences of functional type of edges contributed to the integrated network.

Figure 5

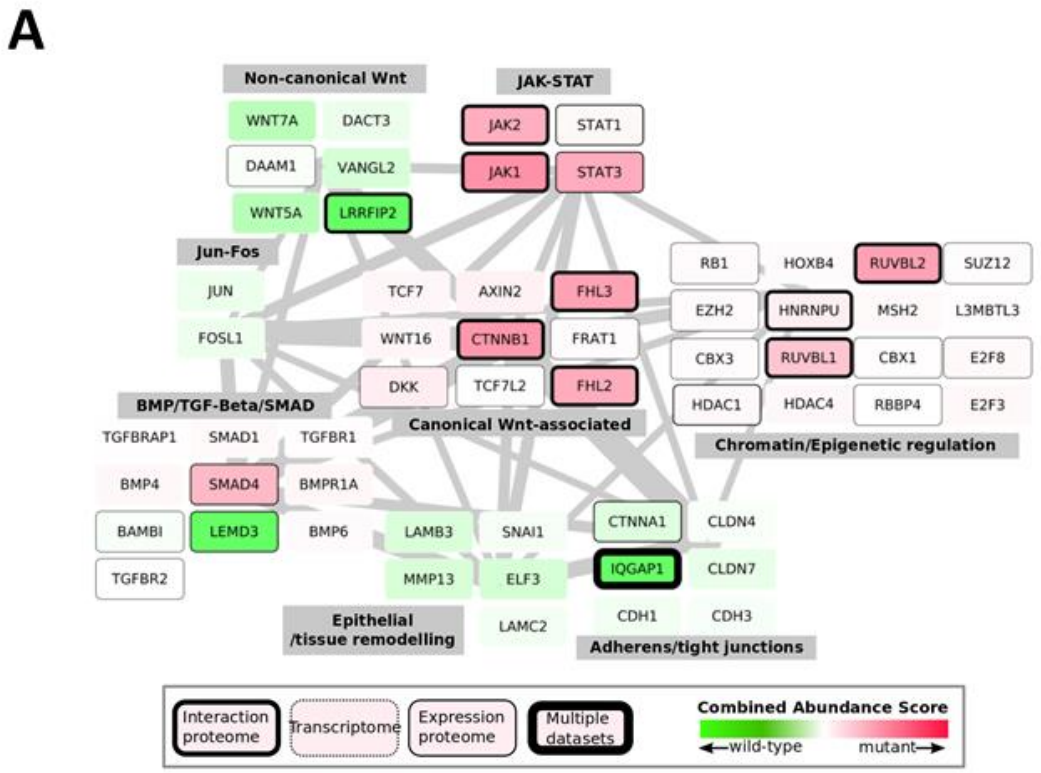
A
Non-canonical Wnt
WNT7A
DACT3
DAAM1
VANGL2
WNT5A
LRRFIP2
JAK-STAT
JAK2
STAT1
JAK1
STAT3
Jun-Fos
JUN
FOSL1
TCF7
AXIN2
FHL3
WNT16
CTNNB1
FRAT1
DKK
TCF7L2
FHL2
Canonical Wnt-associated
BMP/TGF-Beta/SMAD
TGFBRAP1
SMAD1
TGFBR1
BMP4
SMAD4
BMPR1A
BAMBI
LEMD3
BMP6
TGFBR2
LAMB3
SNAI1
MMP13
ELF3
LAMC2
Epithelial
/tissue remodelling
RB1
HOXB4
RUVBL2
SUZ12
EZH2
HNRNPU
MSH2
L3MBTL3
CBX3
RUVBL1
CBX1
E2F8
HDAC1
HDAC4
RBBP4
E2F3
Chromatin/Epigenetic regulation
CTNNA1
CLDN4
IQGAP1
CLDN7
CDH1
CDH3
Adherens/tight junctions
Interaction proteome
Transcriptome
Expression proteome
Multiple datasets
Combined Abundance Score
wild-type
mutant
B
CAND1**
DCUN1D1**
CUL3*
SKP1**
FBXO18*
CACYBP
CTNNB1**
CUL1*

Figure 5 (cont'd)

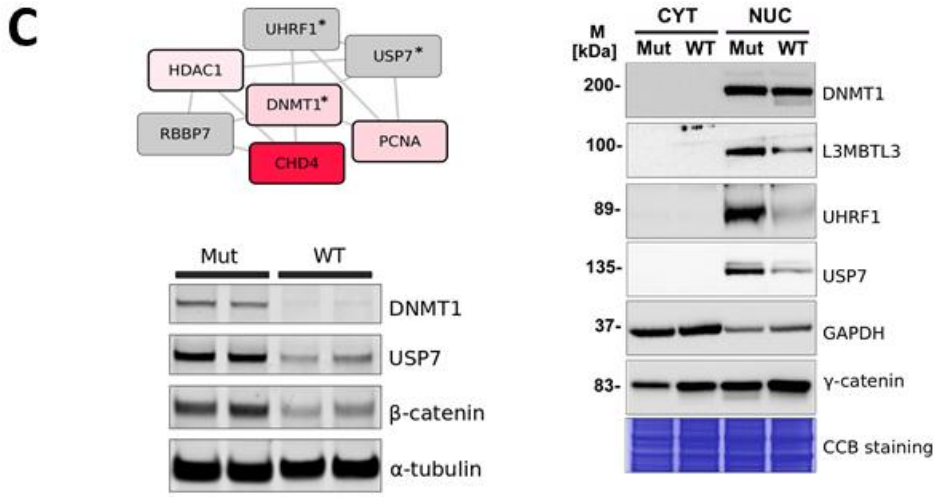

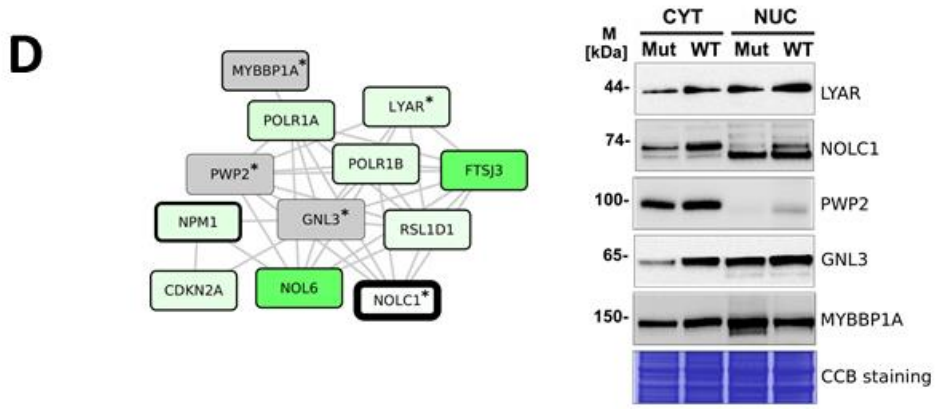

Figure 5 Integrated proteomic and transcriptomic functional modules.

(A) Selected functional modules from the integrated network. Edge thickness represents the overall connectivity between modules (Normalized edge weights calculated as the total number of edges divided by the number of genes/proteins in each module). Node (gene/protein) color intensity indicates the combined abundance score (red = mutant; green = wild-type).

(B) SCF (Skp-Cullin-F-box) associated protein network, showing proteins significantly (** $p<0.05$; * $p<0.1$) abundant in interaction and expression proteome datasets.

(C) DNA methyltransferase I (Dnmt1) associated protein network. Protein nodes marked with an asterisk were also tested by immunoblotting as shown. Dnmt1, USP7 and β-catenin were tested using immunoblotting on whole cell lysates from mutant and wild-type cells and additional related interaction partners (UHRF1, L3MBTL3) analyzed by immunoblotting of nuclear and cytosolic sub-cellular fractions from mutant and wild-type cells.

(D) Western analysis of ribosome biogenesis associated protein network in sub-cellular fractionated samples. Protein nodes marked with asterisk were also tested by immunoblotting as shown in nuclear and cytosolic fractions from mutant and wild-type cells as in Figure 5C.

Supplementary Figure 1

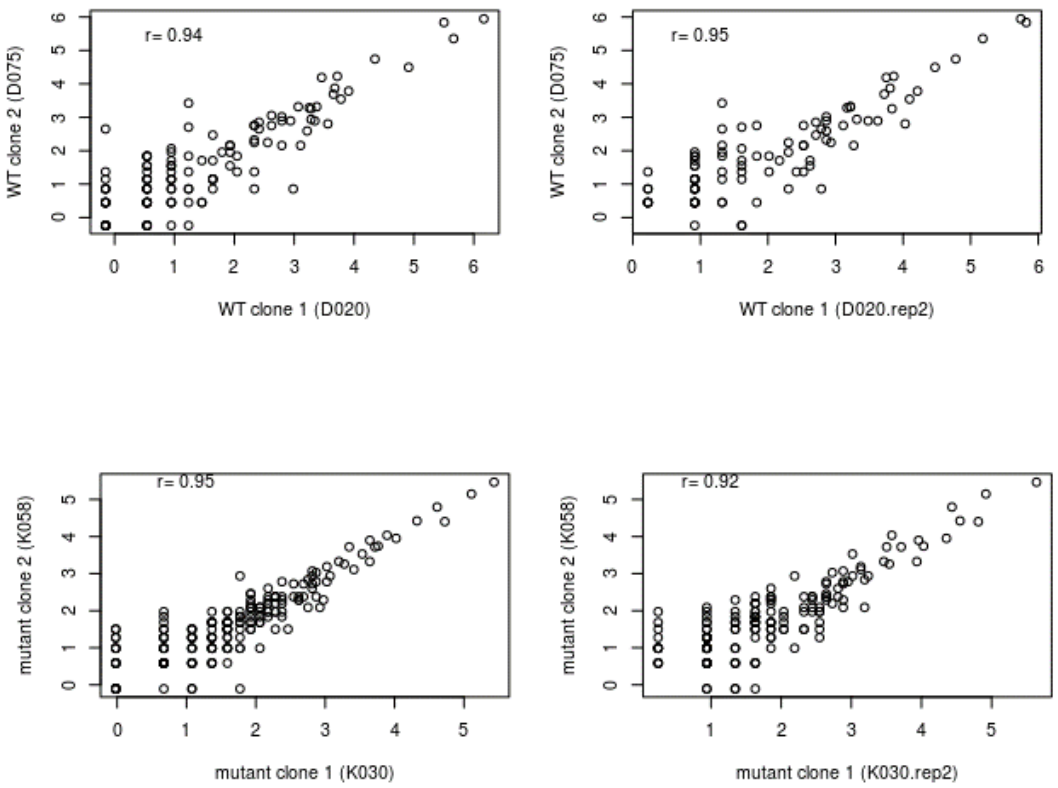

Supplementary Figure 1

Protein abundance (log spectral count values) scatter plots and correlations for AP-MS analyses of separate mutant and wild-type cell-line clones. Plots show proteins present in both compared samples with proteins with high frequency in control samples excluded (upper left panel N=109 proteins; upper right panel N=105 proteins; lower left panel N=151 proteins; lower right panel N=151 proteins).

Supplementary Figure 2

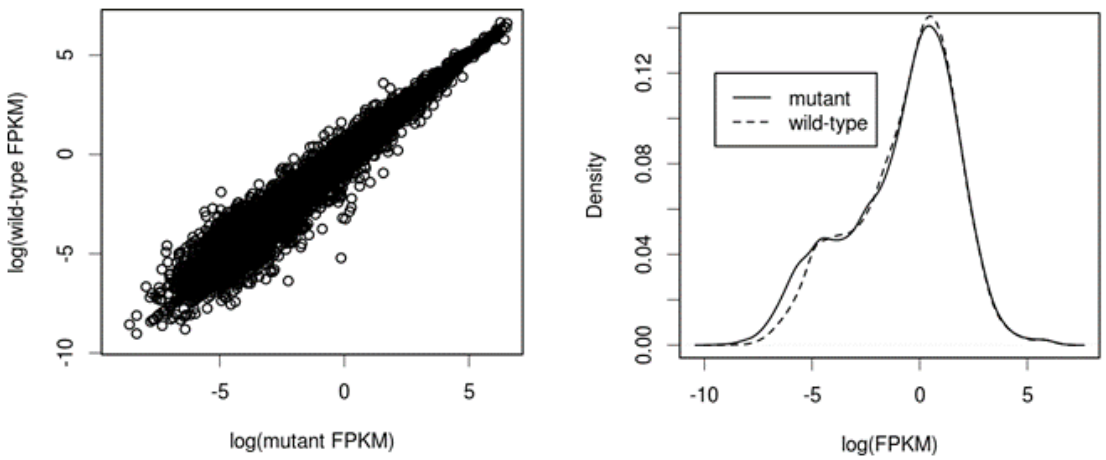

Supplementary Figure 2

Correlation (left figure) and distribution (right) of Fragments Per Kilobase of exon per Million reads (FPKM) values for mutant and wild-type RNA-Seq samples.

Supplementary Figure 3

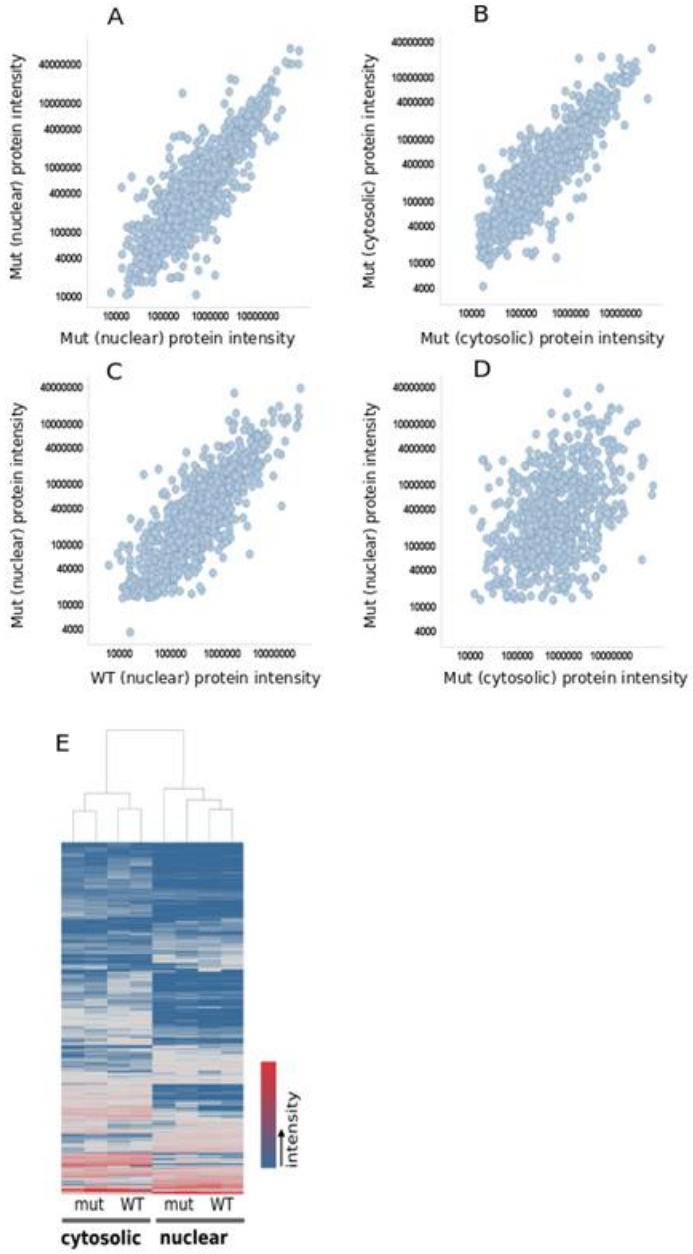

Supplementary Figure 3

Exemplar protein intensity scatter plots (n=3272 proteins) of mutant and wild-type nuclear and cytosolic expression profiling (A) Mutant nuclear vs Mutant nuclear (biological replicate), (B) Mutant cytosolic vs Mutant cytosolic (biological replicate), (C) Mutant nuclear vs wild-type nuclear and (D) Mutant nuclear vs Mutant cytosolic.

(E) Clustered heat map of protein abundance from expression proteome analysis (LC-MS/MS) experiments from mutant (mut) and wild-type (WT) cytosolic or nuclear fractions.

Supplementary Table 4a Peptide list from expression proteomics experiments

Supplementary Table 4b Peptide list from AP-MS proteomics experiments

Supplementary Table 4c Protein and protein group list from expression proteomics experiments

Supplementary Table 4d Protein and protein group list from ap-ms proteomics experiments

Supplementary Table 5 Protein sequence database cross-referencing table for IPI human v3.72

AUTHOR INFORMATION

Corresponding Author

*** for correspondence:** rob.ewing@soton.ac.uk

ACKNOWLEDGMENT

R.M.E and Z.W. acknowledge NCI award 1R21CA16006 that supported in part the work described here. R.M.E acknowledges an EU Marie Curie FP7-PEOPLE-2012-CIG award. This research was supported by the Genomics Core Facility of Case Western Reserve University School of Medicine's Genetics and Genome Sciences Department.

REFERENCES

(1) Clevers, H. Wnt/Beta-Catenin Signaling in Development and Disease. *Cell* **2006**, *127* (3), 469–480.

(2) Amit, S.; Hatzubai, A.; Birman, Y.; Andersen, J. S.; Ben-Shushan, E.; Mann, M.; Ben-Neriah, Y.; Alkalay, I. Axin-Mediated CKI Phosphorylation of Beta-Catenin at Ser 45: A Molecular Switch for the Wnt Pathway. *Genes Dev.* **2002**, *16* (9), 1066–1076.

(3) Morin, P. J.; Sparks, A. B.; Korinek, V.; Barker, N.; Clevers, H.; Vogelstein, B.; Kinzler, K. W. Activation of Beta-Catenin-Tcf Signaling in Colon Cancer by Mutations in Beta-Catenin or APC. *Science* **1997**, *275* (5307), 1787–1790.

(4) Valenta, T.; Hausmann, G.; Basler, K. The Many Faces and Functions of β-Catenin. *EMBO J.* **2012**, *31* (12), 2714–36.

(5) Angers, S.; Moon, R. T. Proximal Events in Wnt Signal Transduction. *Nat. Rev. Mol. Cell Biol.* **2009**.

(6) Cadigan, K. M. TCFs and Wnt/β-Catenin Signaling: More than One Way to Throw the Switch. *Curr. Top. Dev. Biol.* **2012**, *98*, 1–34.

(7) Song, J.; Wang, Z.; Ewing, R. M. Integrated Analysis of the Wnt Responsive Proteome in Human Cells Reveals Diverse and Cell-Type Specific Networks. *Mol. Biosyst.* **2014**, *10* (1), 45–53.

(8) Tian, Q. Proteomic Exploration of the Wnt/Beta-Catenin Pathway. *Curr Opin Mol Ther* **2006**, *8* (3), 191–197.

(9) Gujral, T. S.; MacBeath, G. A System-Wide Investigation of the Dynamics of Wnt Signaling Reveals Novel Phases of Transcriptional Regulation. *PLoS One* **2010**, *5* (4), e10024.

(10) Hilger, M.; Mann, M. Triple SILAC to Determine Stimulus Specific Interactions in the Wnt Pathway. *J Proteome Res* **2011**.

(11) Acebron, S. P.; Karaulanov, E.; Berger, B. S.; Huang, Y.-L.; Niehrs, C. Mitotic Wnt Signaling Promotes Protein Stabilization and Regulates Cell Size. *Mol. Cell* **2014**, *54* (4), 663–674.

(12) Jho, E.; Zhang, T.; Domon, C.; Joo, C.-K.; Freund, J.-N.; Costantini, F. Wnt/Beta-Catenin/Tcf Signaling Induces the Transcription of Axin2, a Negative Regulator of the Signaling Pathway. *Mol Cell Biol* **2002**, *22* (4), 1172–1183.

(13) Niida, A.; Hiroko, T.; Kasai, M.; Furukawa, Y.; Nakamura, Y.; Suzuki, Y.; Sugano, S.; Akiyama, T. DKK1, a Negative Regulator of Wnt Signaling, Is a Target of the [Beta]-Catenin//TCF Pathway. *Oncogene* **2004**, *23* (52), 8520–8526.

(14) Chan, T. A.; Wang, Z.; Dang, L. H.; Vogelstein, B.; Kinzler, K. W. Targeted Inactivation of CTNNB1 Reveals Unexpected Effects of Beta-Catenin Mutation. *Proc Natl Acad Sci U A* **2002**, *99* (12), 8265–8270.

(15) Song, J.; Hao, Y.; Du, Z.; Wang, Z.; Ewing, R. M. Identifying Novel Protein Complexes in Cancer Cells Using Epitope-Tagging of Endogenous Human Genes and Affinity-Purification Mass Spectrometry. *J. Proteome Res.* **2012**, *11* (12), 5630–41.

(16) Nesvizhskii, A. I.; Keller, A.; Kolker, E.; Aebersold, R. A Statistical Model for Identifying Proteins by Tandem Mass Spectrometry. *Anal Chem* **2003**, *75* (17), 4646–58.

(17) Kim, D.; Pertea, G.; Trapnell, C.; Pimentel, H.; Kelley, R.; Salzberg, S. L. TopHat2: Accurate Alignment of Transcriptomes in the Presence of Insertions, Deletions and Gene Fusions. *Genome Biol.* **2013**, *14*, R36.

(18) Anders, S.; Pyl, P. T.; Huber, W. HTSeq—a Python Framework to Work with High-Throughput Sequencing Data. *Bioinformatics* **2015**, *31* (2), 166–169.
(19) Balbin, O. A.; Prensner, J. R.; Sahu, A.; Yocum, A.; Shankar, S.; Malik, R.; Fermin, D.; Dhanasekaran, S. M.; Chandler, B.; Thomas, D.; et al. Reconstructing Targetable Pathways in Lung Cancer by Integrating Diverse Omics Data. *Nat. Commun.* **2013**, *4*.
(20) Chen, E. Y.; Tan, C. M.; Kou, Y.; Duan, Q.; Wang, Z.; Meirelles, G. V.; Clark, N. R.; Ma'ayan, A. Enrichr: Interactive and Collaborative HTML5 Gene List Enrichment Analysis Tool. *BMC Bioinformatics* **2013**, *14*, 128.
(21) Kwon, A. T.; Arenillas, D. J.; Worsley Hunt, R.; Wasserman, W. W. oPOSSUM-3: Advanced Analysis of Regulatory Motif over-Representation across Genes or ChIP-Seq Datasets. *G3 Bethesda Md* **2012**, *2* (9), 987–1002.
(22) Zhao, M.; Sun, J.; Zhao, Z. TSGene: A Web Resource for Tumor Suppressor Genes. *Nucleic Acids Res.* **2013**, *41* (D1), D970–D976.
(23) Chen, J.-S.; Hung, W.-S.; Chan, H.-H.; Tsai, S.-J.; Sun, H. S. In Silico Identification of Oncogenic Potential of Fyn-Related Kinase in Hepatocellular Carcinoma. *Bioinforma. Oxf. Engl.* **2013**, *29* (4), 420–427.
(24) Lin, S. Y.; Xia, W.; Wang, J. C.; Kwong, K. Y.; Spohn, B.; Wen, Y.; Pestell, R. G.; Hung, M. C. Beta-Catenin, a Novel Prognostic Marker for Breast Cancer: Its Roles in Cyclin D1 Expression and Cancer Progression. *Proc. Natl. Acad. Sci. U. S. A.* **2000**, *97* (8), 4262–4266.
(25) Herbst, A.; Jurinovic, V.; Krebs, S.; Thieme, S. E.; Blum, H.; Göke, B.; Kolligs, F. T. Comprehensive Analysis of β-Catenin Target Genes in Colorectal Carcinoma Cell Lines with Deregulated Wnt/β-Catenin Signaling. *BMC Genomics* **2014**, *15*, 74.
(26) Mokry, M.; Hatzis, P.; Schuijers, J.; Lansu, N.; Ruzius, F.-P.; Clevers, H.; Cuppen, E. Integrated Genome-Wide Analysis of Transcription Factor Occupancy, RNA Polymerase II Binding and Steady-State RNA Levels Identify Differentially Regulated Functional Gene Classes. *Nucleic Acids Res.* **2012**, *40* (1), 148–158.
(27) Buck, A.; Buchholz, M.; Wagner, M.; Adler, G.; Gress, T.; Ellenrieder, V. The Tumor Suppressor KLF11 Mediates a Novel Mechanism in Transforming Growth Factor Beta-Induced Growth Inhibition That Is Inactivated in Pancreatic Cancer. *Mol. Cancer Res. MCR* **2006**, *4* (11), 861–872.
(28) Ghaleb, A. M.; Elkarim, E. A.; Bialkowska, A. B.; Yang, V. W. KLF4 Suppresses Tumor Formation in Genetic and Pharmacological Mouse Models of Colonic Tumorigenesis. *Mol. Cancer Res. MCR* **2016**.
(29) Zhao, W.; Hisamuddin, I. M.; Nandan, M. O.; Babbin, B. A.; Lamb, N. E.; Yang, V. W. Identification of Krüppel-like Factor 4 as a Potential Tumor Suppressor Gene in Colorectal Cancer. *Oncogene* **2004**, *23* (2), 395–402.
(30) Zhang, W.; Chen, X.; Kato, Y.; Evans, P. M.; Yuan, S.; Yang, J.; Rychahou, P. G.; Yang, V. W.; He, X.; Evers, B. M.; et al. Novel Cross Talk of Kruppel-like Factor 4 and Beta-Catenin Regulates Normal Intestinal Homeostasis and Tumor Repression. *Mol. Cell. Biol.* **2006**, *26* (6), 2055–2064.
(31) Evans, P. M.; Chen, X.; Zhang, W.; Liu, C. KLF4 Interacts with Beta-Catenin/TCF4 and Blocks p300/CBP Recruitment by Beta-Catenin. *Mol. Cell. Biol.* **2010**, *30* (2), 372–381.
(32) Shah, M.; Rennoll, S. A.; Raup-Konsavage, W. M.; Yochum, G. S. A Dynamic Exchange of TCF3 and TCF4 Transcription Factors Controls MYC Expression in Colorectal Cancer Cells. *Cell Cycle Georget. Tex* **2015**, *14* (3), 323–332.

(33) Gonzalez, D. M.; Medici, D. Signaling Mechanisms of the Epithelial-Mesenchymal Transition. *Sci. Signal.* **2014**, *7* (344), re8.
(34) Pierce, N. W.; Lee, J. E.; Liu, X.; Sweredoski, M. J.; Graham, R. L. J.; Larimore, E. A.; Rome, M.; Zheng, N.; Clurman, B. E.; Hess, S.; et al. Cand1 Promotes Assembly of New SCF Complexes Through Dynamic Exchange of F-Box Proteins. *Cell* **2013**, *153* (1), 206–215.
(35) Song, J.; Du, Z.; Ravasz, M.; Dong, B.; Wang, Z.; Ewing, R. M. A Protein Interaction between -Catenin and Dnmt1 Regulates Wnt Signaling and DNA Methylation in Colorectal Cancer Cells. *Mol. Cancer Res.* **2015**, *13* (6), 969–981.
(36) Du, Z.; Song, J.; Wang, Y.; Zhao, Y.; Guda, K.; Yang, S.; Kao, H.-Y.; Xu, Y.; Willis, J.; Markowitz, S. D.; et al. DNMT1 Stability Is Regulated by Proteins Coordinating Deubiquitination and Acetylation-Driven Ubiquitination. *Sci Signal* **2010**, *3* (146), ra80.
(37) Qin, W.; Leonhardt, H.; Pichler, G. Regulation of DNA Methyltransferase 1 by Interactions and Modifications. *Nucl. Austin Tex* **2011**, *2* (5), 392–402.
(38) Stott, F. J.; Bates, S.; James, M. C.; McConnell, B. B.; Starborg, M.; Brookes, S.; Palmero, I.; Ryan, K.; Hara, E.; Vousden, K. H.; et al. The Alternative Product from the Human CDKN2A Locus, p14(ARF), Participates in a Regulatory Feedback Loop with p53 and MDM2. *EMBO J.* **1998**, *17* (17), 5001–5014.
(39) Tsai, R. Y. L. Turning a New Page on Nucleostemin and Self-Renewal. *J. Cell Sci.* **2014**, *127* (Pt 18), 3885–3891.
(40) Ewing, R. M.; Chu, P.; Elisma, F.; Li, H.; Taylor, P.; Climie, S.; McBroom-Cerajewski, L.; Robinson, M. D.; O'Connor, L.; Li, M.; et al. Large-Scale Mapping of Human Protein-Protein Interactions by Mass Spectrometry. *Mol. Syst. Biol.* **2007**, *3*, 89.
(41) Kikuchi, A.; Yamamoto, H.; Sato, A.; Matsumoto, S. Wnt5a: Its Signalling, Functions and Implication in Diseases. *Acta Physiol.* **2012**, *204* (1), 17–33.
(42) van Amerongen, R.; Fuerer, C.; Mizutani, M.; Nusse, R. Wnt5a Can Both Activate and Repress Wnt/β-Catenin Signaling during Mouse Embryonic Development. *Dev. Biol.* **2012**, *369* (1), 101–114.
(43) Ying, J.; Li, H.; Yu, J.; Ng, K. M.; Poon, F. F.; Wong, S. C. C.; Chan, A. T. C.; Sung, J. J. Y.; Tao, Q. WNT5A Exhibits Tumor-Suppressive Activity through Antagonizing the Wnt/Beta-Catenin Signaling, and Is Frequently Methylated in Colorectal Cancer. *Clin. Cancer Res. Off. J. Am. Assoc. Cancer Res.* **2008**, *14* (1), 55–61.
(44) Dejmek, J. Wnt-5a Protein Expression in Primary Dukes B Colon Cancers Identifies a Subgroup of Patients with Good Prognosis. *Cancer Res.* **2005**, *65* (20), 9142–9146.
(45) Novellasdemunt, L.; Foglizzo, V.; Cuadrado, L.; Antas, P.; Kucharska, A.; Encheva, V.; Snijders, A. P.; Li, V. S. W. USP7 Is a Tumor-Specific WNT Activator for APC-Mutated Colorectal Cancer by Mediating β-Catenin Deubiquitination. *Cell Rep.* **2017**, *21* (3), 612–627.
(46) Baylin, S. B.; Herman, J. G.; Graff, J. R.; Vertino, P. M.; Issa, J. P. Alterations in DNA Methylation: A Fundamental Aspect of Neoplasia. *Adv. Cancer Res.* **1998**, *72*, 141–196.
(47) Acebron, S. P.; Niehrs, C. β-Catenin-Independent Roles of Wnt/LRP6 Signaling. *Trends Cell Biol.*
(48) Joyce, A. R.; Palsson, B. Ø. The Model Organism as a System: Integrating "Omics" Data Sets. *Nat. Rev. Mol. Cell Biol.* **2006**, *7* (3), 198–210.